Inhibition of thermophilic F₁-ATPase by the ε subunit takes different path from the ADP-Mg inhibition

Takamitsu Haruyama[1,2], Yoko Hirono-Hara[3] and Yasuyuki Kato-Yamada[1,2]

[1]*Department of Life Science, Rikkyo University, 3-34-1, Nishi-Ikebukuro, Toshima-ku, Tokyo 171-8501, Japan*
[2]*Frontier Project "Adaptation and Evolution of Extremophile", College of Science, Rikkyo University, 3-34-1, Nishi-Ikebukuro, Toshima-ku, Tokyo 171-8501, Japan*
[3]*Institute of Industrial Science, the University of Tokyo, 4-6-1, Komaba, Meguro-ku, Tokyo 153-8505, Japan*

The F₁-ATPase, the soluble part of FoF₁-ATP synthase, is a rotary molecular motor consisting of $\alpha_3\beta_3\gamma\delta\epsilon$. The γ and ϵ subunits rotate relative to the $\alpha_3\beta_3\delta$ sub-complex on ATP hydrolysis by the β subunit. The ϵ subunit is known as an endogenous inhibitor of the ATPase activity of the F₁-ATPase and is believed to function as a regulator of the ATP synthase. This inhibition by the ϵ subunit (ϵ inhibition) of F₁-ATPase from thermophilic *Bacillus* PS3 was analyzed by single molecule measurements. By using a mutant ϵ subunit deficient in ATP binding, reversible transitions between active and inactive states were observed. Analysis of pause and rotation durations showed that the ϵ inhibition takes a different path from the ADP-Mg inhibition. Furthermore, the addition of the mutant ϵ subunit to the $\alpha_3\beta_3\gamma$ sub-complex was found to facilitate recovery of the ATPase activity from the ADP-Mg inhibition. Thus, it was concluded that these two inhibitions are essentially exclusive of each other.

Key words: ATP synthase, ADP inhibited form, regulation

The FoF₁-ATPase/synthase (FoF₁) is a rotary molecular motor that consists of water-soluble ATP-driven F₁ and membrane-embedded H⁺- or Na⁺-driven Fo and couples ATP synthesis/hydrolysis and ion flow[1,2]. Its rotation has been studied by direct observation at the single-molecule level and details of the rotary catalytic mechanism have

been revealed[3–5]. The F₁-ATPase ($\alpha_3\beta_3\gamma\delta\epsilon$) hydrolyzes ATP into ADP and Pi and the hydrolysis of one ATP drives a discrete 120° rotation of the $\gamma\epsilon$ subunits relative to the other subunits. The 120° step can be resolved into an 80° sub-step initiated by the ATP-binding and a 40° sub-step initiated by the release of one of the reaction products, Pi. This sequence of events can be summarized as "ATP-binding dwell", "80° stepping rotation", "catalytic dwell", and "40° stepping rotation".

The ϵ subunit, the smallest subunit of F₁-ATPase, is known as an endogenous inhibitor of the ATPase activity of bacterial and chloroplast F₁. Although the inhibition by the ϵ subunit (ϵ inhibition) is common, the mechanism behind it varies considerably among species. In F₁-ATPases from *Escherichia coli* (EF₁) and from chloroplast (CF₁), when F₁-ATPase is separated from Fo, the ϵ subunit functions as a dissociative inhibitor: The ϵ subunit inhibits the ATPase activity just by the binding and the inhibition is controlled by dissociation/association of the ϵ subunit from the F₁-ATPase[6–8]. Consequently, the presence of excess ϵ subunit strengthens the inhibition. In contrast, the ϵ subunit of F₁-ATPase from thermophilic *Bacillus* PS3 (TF₁) does not dissociate from the TF₁ complex and, thus, excess ϵ hardly affects the ATPase activity[9]. The ϵ inhibition in TF₁ is controlled by a change of the conformation of the ϵ subunit. When the ϵ subunit is in an extended-state conformation, it inserts its C-terminal α helices into the cavity of the $\alpha_3\beta_3$ ring and inhibits the ATPase activity[10–12]. When the ϵ subunit is in an intermediate-state conformation, in which the C-terminal α helices of the ϵ subunit are withdrawn out of the $\alpha_3\beta_3$ ring, the ATPase activity is not inhibited. This uninhibited state of the ATPase is stabilized by the ATP

Corresponding author: Yasuyuki Kato-Yamada, Department of Life Science, College of Science, Rikkyo University, 3-34-1, Nishi-Ikebukuro, Toshima-ku, Tokyo 171-8501, Japan.
e-mail: katoyama@rikkyo.ac.jp

binding to the ε subunit, which is called folded-state conformation, with its C-terminal α helices folded into a helix-turn-helix conformation. This mechanism has been supported by a number of biochemical studies[10–13].

The F_1-ATPase is also known to be inhibited by ADP-Mg trapped in the catalytic site(s), which has been termed as the ADP-Mg inhibition (or the ADP inhibition). All the F_1-ATPases thus far examined have been shown to be subject to this mode of inhibition. Recovery from the ADP-Mg inhibited state is accelerated by the binding of ATP to the non-catalytic site(s) on the α subunits[14,15]. Single-molecule study has shown that the ADP-Mg inhibition can be observed as pauses of the rotation[16]. The pause angle of the γ subunit during the ADP-Mg inhibition is the same as that of the catalytic dwell, namely, 80° from the ATP-binding dwell.

Several previous studies have proposed that the ε inhibition stabilizes the ADP-Mg inhibited state[17–19]. However, the ε inhibition is effective even in the presence of a detergent, lauryldimethylamine oxide (LDAO), which is known to weaken the ADP-Mg inhibition[12]. Our previous study indicated that the ε subunit greatly reduces the affinity of ADP-Mg to the catalytic sites: the ε subunit may actually counteract the ADP-Mg inhibition[20].

In order to examine the relationship between the ε inhibition and the ADP-Mg inhibition, we have carried out single-molecule analysis of the effects of the ε subunit on the rotation of TF_1 and measurement of the ATPase activity of TF_1 in the present study. Previously, observation of repetitive transitions between active and ε inhibited states was limited to a very low concentration of ATP (200 nM), because the wild-type ε subunit binds ATP very strongly at room temperature[19]. In the present study, use of a mutant ε subunit deficient in ATP binding made the observation possible even with 200 μM ATP, allowing us to carry out detailed analyses. The results indicated that the ε inhibition and the ADP-Mg inhibition are essentially exclusive of each other.

Materials and Methods

Materials — A mutant (αC193S, βHis$_{10}$ at N-terminus, and γS107C) $α_3β_3γ$ sub-complex of TF_1-ATPase (TF_1(-ε)) was labeled at a cystein on the γ subunit by biotin-$PEAC_5$-maleimide (Dojin, Japan) as described[16]. The ΔNC mutant $α_3β_3γ$ sub-complex of TF_1-ATPase, which contains αK175A/T176A mutations in addition to the above mutations, was prepared as described[14,16]. Wild-type and R126A mutant ε subunits of TF_1 were prepared as described[13,21]. The nucleotide content of the ε subunit was estimated by UV absorption spectrum to be less than 0.05 mol of ATP/mol of ε[22]. The $α_3β_3γε$ sub-complex used in the ATPase measurement was reconstituted from the $α_3β_3γ$ sub-complex and the ε subunit prior to use by simple mixing at an approximate molar ratio of $α_3β_3γ : ε = 1 : 10$. ATP was purchased from Wako Chemicals. Phospho*enol*pyruvate was purchased from Sigma-Aldrich. Streptavidin coated magnetic beads (0.73 μm) were purchased from Seradyn (Indianapolis). Pyruvate kinase and lactate dehydrogenase were purchased from Roche Diagnostics. Other chemicals were of the highest grades available.

Rotation assay — A flow cell was constructed from a bottom cover glass coated with Ni^{2+}-NTA, an uncoated top cover glass, and spacers of ca. 100 μm thickness[16]. F_1 at 5.4 nM (with or without 90 nM $ε^{WT}$ or 120 nM $ε^{R126A}$) in 50 mM MOPS-KOH (pH 7.0) and 50 mM KCl was infused into the flow cell. After 2 min, the flow cell was washed with buffer A (50 mM MOPS-KOH (pH 7.0), 50 mM KCl, 2 mM $MgCl_2$ and 1% bovine serum albumin) and the magnetic beads were infused. After 10 min, the unbound beads were washed out with buffer A and buffer A containing various concentrations of ATP-Mg and an ATP-regenerating system (50 μg/ml of pyruvate kinase and 2.5 mM phospho*enol*pyruvate) was infused. Although the binding of TF_1(-ε) and ε is known to be strong enough[9], excess ε subunit (1 μM) was also included to avoid possible loss of the ε subunit. Rotating beads (or broken pieces thereof) were observed in the bright field mode on an inverted microscope (IX-71, Olympus) with a 100× objective. The images were recorded at the video rate (30 fps) by a full-frame charge-coupled device camera equipped with a high speed shutter (FC-300M, TAKEX, Tokyo) and recorded on a digital video recorder (DSR-45A, Sony, Tokyo). The shutter speed was set to 1/30 s. The images of the beads were analyzed by a custom-made software (Ryohei Yasuda, Duke University, Durham, NC)[3].

Pause analysis — The pausing periods longer than 1 s were defined as the inactive state. The rotating periods between successive inactive states were defined as the active state. The durations of the inactive and the active states were measured.

ATPase assay — ATPase activity was measured spectrophotometrically with an ATP-regenerating system coupled to NADH oxidation at 25°C[23]. The assay mixture consisted of 50 mM MOPS-KOH (pH 7.0), 50 mM KCl, 2.5 mM phospho*enol*pyruvate, 2 mM $MgCl_2$, 0.2 mM NADH, 50 μg/ml pyruvate kinase, 50 μg/ml lactate dehydrogenase, and various concentrations of ATP-Mg. The reaction was initiated by the addition of 1.7 to 6.8 nM of biotinylated subunit complexes of TF_1 to the assay mixture, and the changes in the absorbance at 340 nm were measured on a spectrophotometer V-550 (JASCO, Tokyo). The ATPase activity was calculated by the kinetics during 1010–1110 s after the initiation of the reaction. For measurement with TF_1(ΔNC), the concentration of the TF_1(ΔNC) was 36 nM.

Other methods — The concentration of ε was determined by the Bradford method[24] with a correction factor of 0.54[22]. The concentration of F_1 was determined by UV absorption with a molar extinction coefficient of F_1, 154,000 at 280 nm.

Results and Discussion

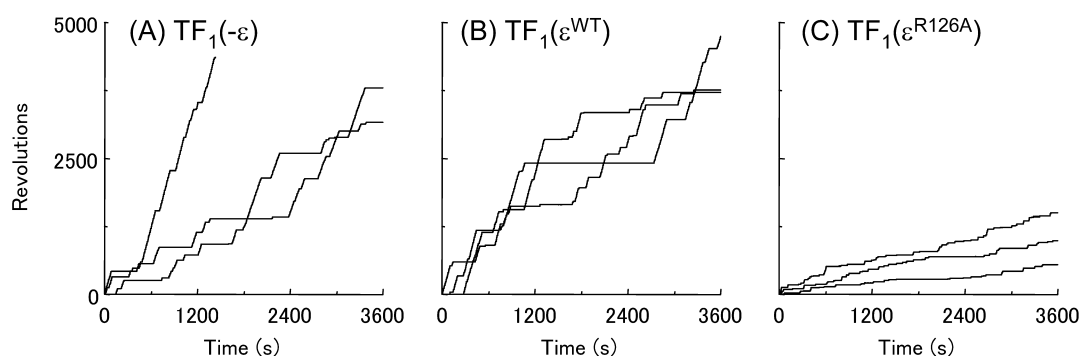*Reversible inhibition of TF_1 by the ε subunit* — It has

Figure 1 Time-course of the rotation of beads attached to TF$_1$(-ε), TF$_1$(ε^{WT}) and TF$_1$(ε^{R126A}). Typical examples of time-course of bead rotation at 200 μM ATP with (A) TF$_1$(-ε), (B) TF$_1$(ε^{WT}) and (C) TF$_1$(ε^{R126A}) are shown. Data with similar bead sizes are shown.

been proposed that ATP binding to the ε subunit of TF$_1$ stabilizes its folded-state conformation, with which TF$_1$ is in the ATPase-active state[13]. As shown in Figure 1, TF$_1$ with the wild-type ε subunit (TF$_1$(ε^{WT})) showed essentially the same rotational behavior as the TF$_1$ lacking ε subunit (TF$_1$(-ε)). Because the ATP binding to the wild-type ε subunit is very strong with a K_d in the order of μM at room temperature[12,13], once the ATPase is activated, it does not return to the ε inhibited state, when the ATP concentration is higher than the K_d. Use of a mutant ε subunit (ε^{R126A}), which is essentially deficient in ATP binding with a K_d larger than 1 mM[13], allowed observation of reversible transition of TF$_1$ into the ε inhibited state even with high concentrations of ATP (200 μM). The overall rotational rate of the TF$_1$(ε^{R126A}) was clearly slower (Fig. 1). In a previous study, it was only at extremely low concentrations of ATP that such transitions were observed with TF$_1$(ε^{WT})[19]. It should be noted that reversible transitions, such as observed here with the mutant ε^{R126A}, are physiologically relevant, because the ATP binding to the wild-type ε subunit is weak at 65°C[12], a physiological temperature of the *Bacillus* PS3. The repetitive transitions between the active and the inactive states allowed us to evaluate the lifetimes of the states. The distributions of the durations of the inactive state (pauses longer than 1 s) and of the active state (the state in between successive inactive states) are shown in Figures 2 and 3, respectively. Their lifetimes were estimated by fitting each panel of the data with a function with one or two exponentials (Figs. 2 and 3 and Table 1). The lifetimes of the inactive state (τ_{i1} and τ_{i2}) were essentially the same among TF$_1$(-ε), TF$_1$(ε^{WT}), and TF$_1$(ε^{R126A}) for various concentrations of ATP (Fig. 2 and Table 1). The inactive state observed with TF$_1$(-ε) was the ADP-Mg inhibition, because the ATPase lacked the ε subunit. The inactive state observed with TF$_1$(ε^{WT}) must have been also the ADP-Mg inhibition, because ε^{WT} must have been in the folded-state conformation with bound ATP at the ATP concentrations employed.

Two exponentials were necessary to fit the data of the inactive state durations. The lifetimes were basically in agreement with those previously reported for the ADP-Mg

Table 1 Time constants for active/inactive state durations

Sample, ATP (μM)	active (τ_a, s)	inactive1[a] (τ_{i1}, s)	inactive2[b] (τ_{i2}, s)
TF$_1$(-ε), 20	13	65	3.9
TF$_1$(-ε), 200	16	35	2.9
TF$_1$(-ε), 2000	11	23	3.7
TF$_1$(ε^{WT}), 20	16	26	–[c]
TF$_1$(ε^{WT}), 200	14	80	5.3
TF$_1$(ε^{WT}), 2000	17	33	5.0
TF$_1$(ε^{R126A}), 20	0.6	72	23
TF$_1$(ε^{R126A}), 200	2.2	39	6.5
TF$_1$(ε^{R126A}), 2000	14	35	4.5

[a,b] Inactive1 and inactive2 represent slower and faster time constants, respectively.
[c] Not determined due to no convergence.

inhibition[16]. The short lived inactive state (corresponding to τ_{i2}) was also observed as in a previous study. Although a slightly larger value was obtained for τ_{i2} with TF$_1$(ε^{R126A}) at 20 μM ATP (Fig. 2 and Table 1), we focus only on τ_{i1} here, as in the previous study[16]. In contrast to the relative insensitivity of the lifetimes of the inactive state to the presence and the kind of the ε subunit or to the ATP concentration, the lifetime of the active state (τ_a) for TF$_1$(ε^{R126A}) was different from that of TF$_1$(-ε) or TF$_1$(ε^{WT}) and depended on the ATP concentration (Fig. 3 and Table 1). It was shorter than that with TF$_1$(-ε) or TF$_1$(ε^{WT}) by over 10 fold at 20 μM ATP. As the ATP concentration was raised, the lifetime became longer, reaching the same level with TF$_1$(-ε) or TF$_1$(ε^{WT}) at 2 mM ATP. According to the previously proposed model that the ε subunit stabilizes the ADP-Mg inhibition[18,19] and the ADP-Mg inhibition is prerequisite for the ε inhibition[19], the lifetime of the active state should not be shortened by the presence of the ε subunit, while the lifetime of the inactive state could be affected. Thus, this has led us to consider an alternative scheme where the ε inhibition and the ADP-Mg inhibition are the parallel paths (Fig. 4). With this scheme, it can be estimated that most (ca. 86%) of the inhibited states of the TF$_1$(ε^{R126A}) with 200 μM ATP must be by the ε. Distinction between the two inhibited states, apart from kinetic arguments, is currently not feasible, because
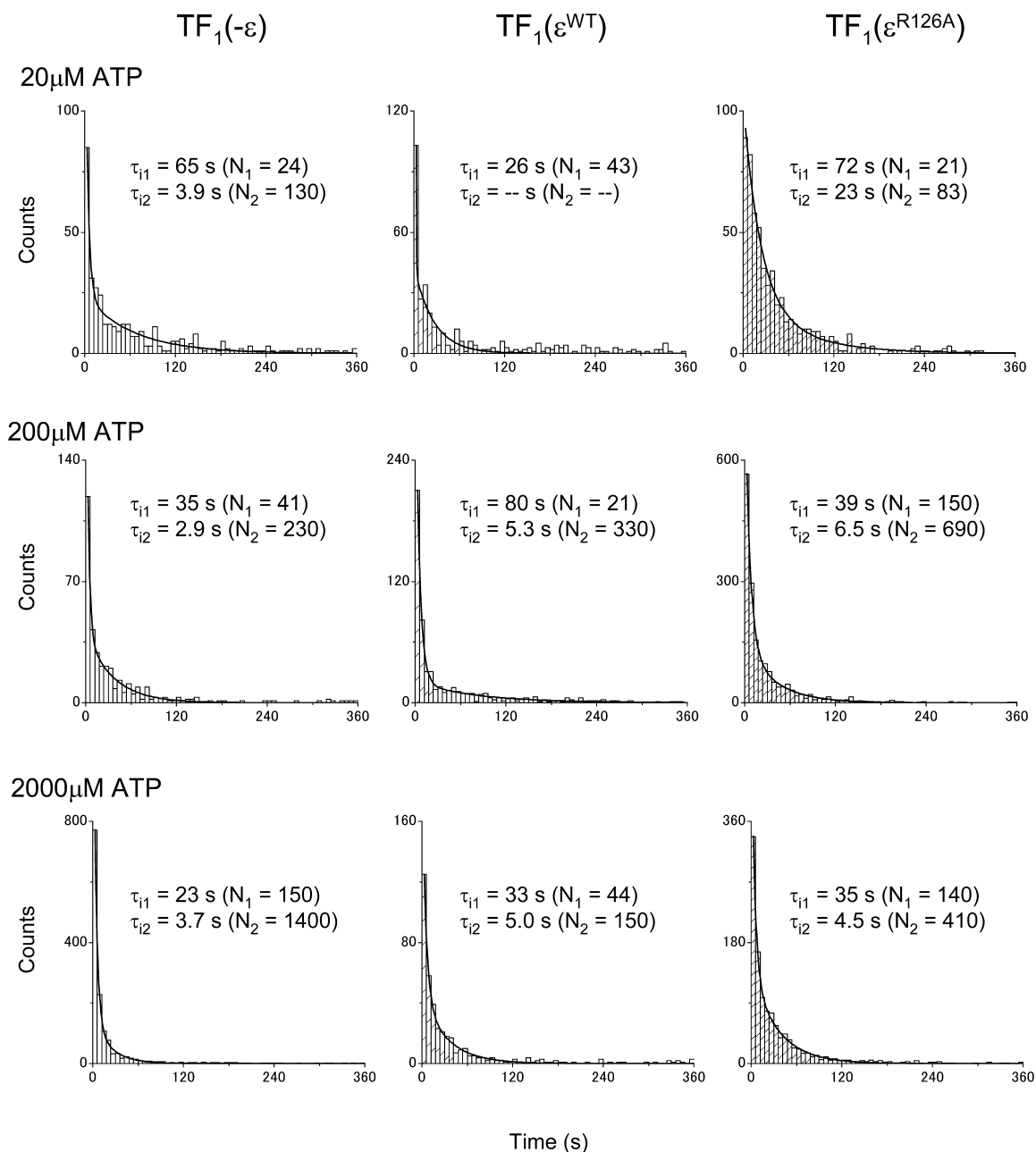
Figure 2 Distribution of inactive state durations. The durations of the inactive state were measured and their distributions are shown. Samples used are indicated on the top of each column. The ATP concentrations were 20 μM, 200 μM, and 2 mM, respectively from the top to the bottom rows. Each distribution was fitted with the sum of two exponential functions: $y = N_1 \exp(-t/\tau_{i1}) + N_2 \exp(-t/\tau_{i2})$. The best-fit values of τ_{i1}, τ_{i2}, N_1, and N_2 are shown on each panel. Solid lines show the best-fit curves. τ_{i2} and N_2 for $TF_1(\varepsilon^{WT})$ with 20 μM ATP could not be obtained due to no convergence.

the angular position of the γ subunit in the ε inhibition and that in the ADP-Mg inhibition are the same (data not shown), which supports a previous proposal[17,19].

The kinetic constants obtained by our analysis (Table 1) are not far from those expected from biochemical experiments[12]. The occupancy of the active-state ((sum of durations of the active states) / (sum of durations of the inactive and the active states)) was calculated for $TF_1(\varepsilon^{R126A})$ and divided by that of $TF_1(-\varepsilon)$. This ratio had a dependence on

the ATP concentration which was similar to the ATP dependence of the relative ATPase activity of $TF_1(\varepsilon^{R126A})$ to $TF_1(-\varepsilon)$ (Fig. 5). The agreement shows that the results by the two methods are consistent. However, our values are different from those reported by Tsumuraya et al.[19]. According to their report, the ε subunit prolonged the duration of the inactive state by 6 fold (from 110 s to 670 s) and the active state was not affected significantly (from 300 to 330 s) at 200 nM ATP[19]. On the basis of the reported apparent second-order
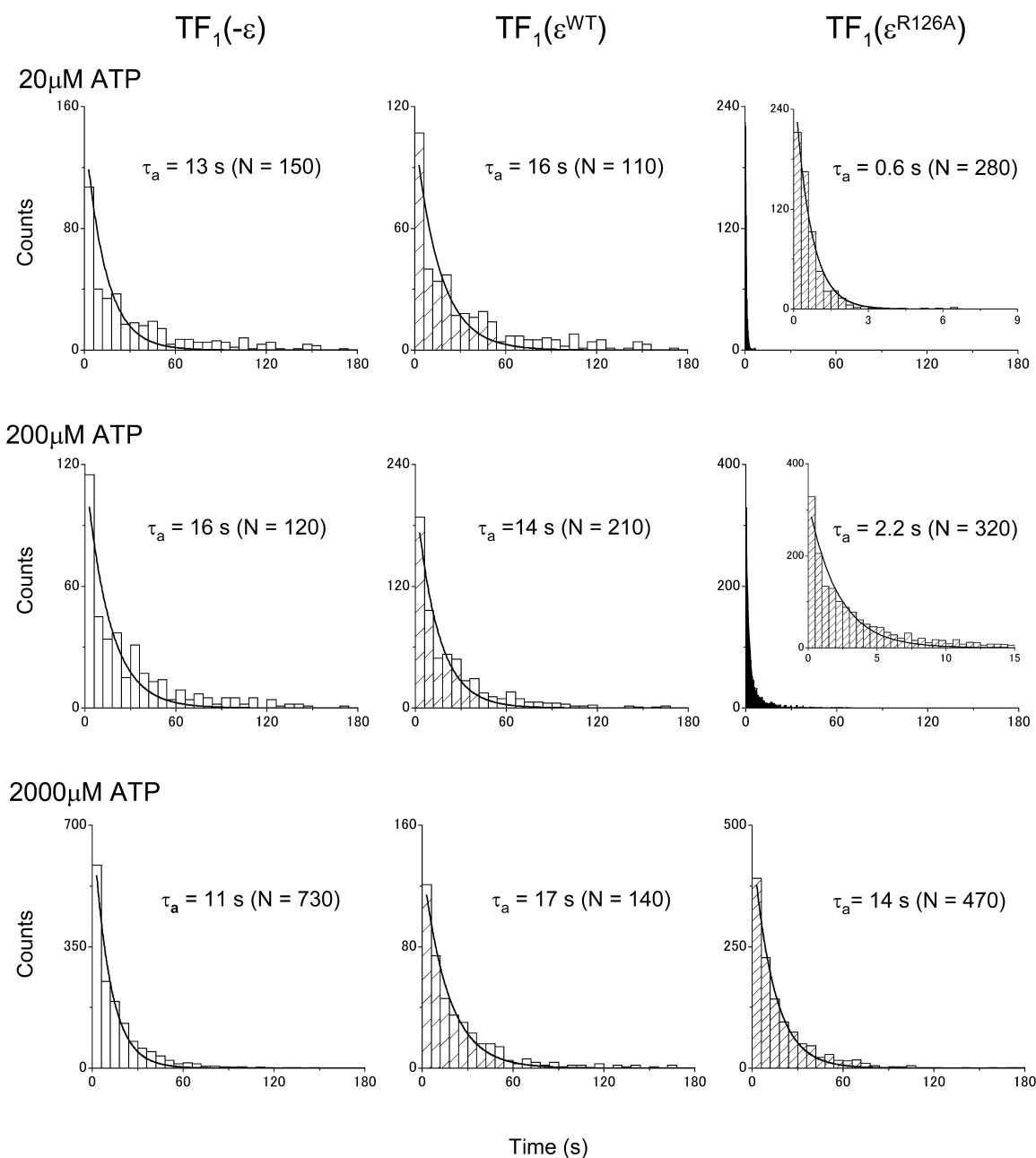
Figure 3 Distribution of active state durations. The durations of the active state were measured and their distributions are shown. Samples used are indicated on the top of each column. The ATP concentrations were 20 μM, 200 μM, and 2 mM, respectively from the top to the bottom rows. Each distribution was fitted with a single exponential function: $y = N \exp(-t/\tau_a)$. The best-fit values of τ_a and N are shown on each panel. Solid lines show the best-fit curves. Insets in TF(ε^{R126A}) with 20 and 200 μM are enlargements along the x-axis.

rate constant for activation[12], the activation of the ε inhibited TF$_1$(ε^{WT}) is estimated to take about 3 days with 200 nM ATP and should not have been observable at the ATP concentration. As Tsumuraya *et al.* pre-incubated TF$_1$(ε^{WT}) in a high concentration of ATP, which was necessary to observe the rotation of TF$_1$(ε^{WT}) at low concentrations of ATP, the ε subunit in their study may have retained ATP and what was observed may have been the differences in the ADP-Mg inhibition between TF$_1$(-ε) and TF$_1$(ε^{WT} with bound ATP)

rather than those in the ε inhibition.

Effect of ε subunit on ATPase activity of TF$_1$(ΔNC) — TF$_1$ comprising the K175A/T176A double mutant of the α subunit, TF$_1$(ΔNC), lacks the nucleotide binding ability of the non-catalytic sites on α subunits and its ADP-Mg inhibition is known to be very strong[15] (recovery from F$_1$*ADP-Mg hardly occurs). To examine further the relationship between the ε inhibition and the ADP-Mg inhibition, the effect of the ε subunit on the ATPase activity of TF$_1$(ΔNC) was examined.
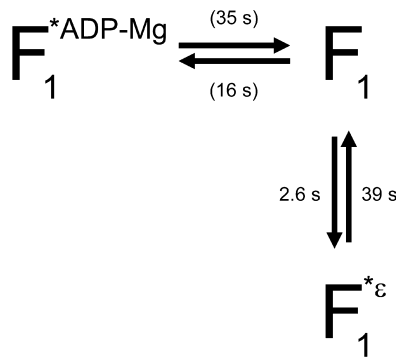
Figure 4 Schematic model of the relationship between ε inhibition and ADP-Mg inhibition. F_1, $F_1^*\varepsilon$ and F_1^*ADP-Mg represent F_1 in active state, ε inhibited state and ADP-Mg inhibited state, respectively. The time constant for each path at 200 μM ATP is shown. The time constant for recovery from ε inhibition was taken from τ_{il} for $TF_1(\varepsilon^{R126A})$. Values shown in parentheses, which represent time constants for the ADP-Mg inhibition, are from τ_a and τ_{il} for $TF_1(-\varepsilon)$. The time constant for the ε inhibition is calculated as $1/(1/\tau_a(TF_1(\varepsilon^{R126A})) - 1/\tau_a(TF_1(-\varepsilon)))$ assuming that $\tau_a(TF_1(\varepsilon^{R126A}))$ contained contributions both from the ε inhibition and from the ADP-Mg inhibition ($\tau_a(TF_1(-\varepsilon))$).

Figure 6 Activation of $TF_1(\Delta NC)$ by the addition of ε^{R126A}. The ATPase activity of $TF_1(\Delta NC)$ was measured by the decrease of absorbance at 340 nm using the NADH-coupled ATP-regenerating system at 50 μM ATP. The reaction was initiated by the addition of $TF_1(\Delta NC)$ lacking ε at the time indicated by the left arrowhead. ε^{WT}, ε^{R126A} (360 nM), or buffer (-ε), was added at the time indicated by the right arrowhead. Vertical and horizontal bars denote 0.01 absorbance and 200 s, respectively.
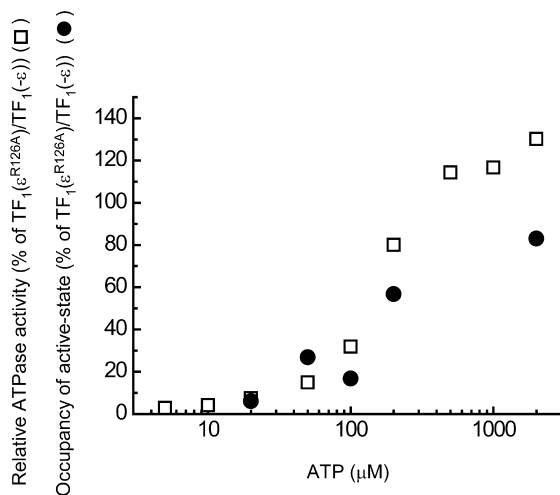

Figure 5 Comparison of relative ATPase activity and occupancy of the active state. The occupancy of the active state was the sum of the durations in the active state divided by the same sum plus the sum for the inactive state. The obtained occupancy for $TF_1(\varepsilon^{R126A})$ was divided by that for $TF_1(-\varepsilon)$ and plotted against the ATP concentration (closed circles). ATPase activity of $TF_1(\varepsilon^{R126A})$ was divided by that of $TF_1(-\varepsilon)$ and plotted against the ATP concentration (open squares).

If the ε inhibition is through stabilization of the ADP-Mg inhibition, addition of ε should result in even stronger inhibition. The results are shown in Figure 6. $TF_1(\Delta NC)$ showed a very low ATPase activity, as previously reported[15]. Although no effect on the ATPase activity was observed with ε^{WT}, when ε^{R126A} was added, recovery of the ATPase activity was observed, contrary to the above prediction (Fig. 6). Because the activation is specific to the mutant ε that is essentially deficient in ATP binding, it is likely that
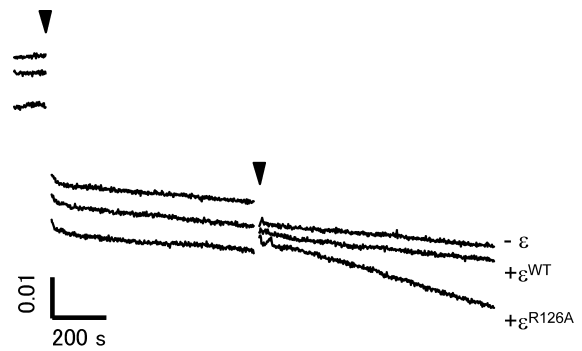
the extended-state conformation of the C-terminal domain is involved in $TF_1(\Delta NC)$'s escape from ADP-Mg inhibition. The extended-state conformation of the ε subunit is known to reduce the affinity of the catalytic sites of TF_1 to ADP by 1 to 3 orders of magnitude[20]. The conformational change of the ε subunit in the ADP-Mg inhibited F_1 (F_1^*ADP-Mg in Fig. 4) from the intermediate- to the extended-states may facilitate direct escape from the ADP-Mg inhibited state (F_1^*ADP-Mg) to the ε inhibited state ($F_1^*\varepsilon$) (a route not shown in Fig. 4), resulting in the recovery of the ATPase activity of $TF_1(\Delta NC)$ though weak (Fig. 6).

Comparison with F_1-ATPases from other sources — Nakanishi-Matsui *et al.* have reported that the ε subunit of EF_1 made frequent pauses during observation of the rotation in the ms order time scale[25]. This is consistent with the EF_1 ε subunit being a non-competitive inhibitor that reduces the V_{max} value of the EF_1 (-ε)[26,27]. Konno *et al.* have reported results of single-molecule analysis on the ε inhibition of cyanobacterial F_1-ATPase[17]. The inhibition was in an on/off fashion accompanying association and dissociation of the ε subunit. The position of the γ subunit arrested in the ε inhibited state was the same as that in the ADP-Mg inhibited state. From these results, the authors argued that the ε inhibition might be effective through stabilizing the ADP-Mg inhibition.

However, the present results show that the two modes of inhibition are not closely related and, therefore, it may be a mere coincidence that the γ subunit stops at the same angular position in the two inhibited states. Conclusion must await the determination of the structure of F_1-ATPase with a ε subunit in the extended-state conformation.

In summary, the current study has shown that the ε inhibition takes a different path from the ADP-Mg inhibition. Use of the mutant ε subunit deficient in ATP binding allowed us to carry out precise analyses on the ε inhibition under vari-

ous conditions. Further analysis, e.g., in the presence of high concentrations of ADP or Pi[18], with the mutant ε subunit will clarify the rather complicated regulatory mechanisms of the bacterial ATP synthase.

References

1. Boyer, P. D. The ATP synthase—a splendid molecular machine. *Annu. Rev. Biochem.* **66**, 717–749 (1997).
2. Yoshida, M., Muneyuki, E. & Hisabori, T. ATP synthase—a marvellous rotary engine of the cell. *Nat. Rev. Mol. Cell Biol.* **2**, 669–677 (2001).
3. Yasuda, R., Noji, H., Yoshida, M., Kinosita, K. Jr. & Itoh, H. Resolution of distinct rotational substeps by submillisecond kinetic analysis of F$_1$-ATPase. *Nature* **410**, 898–904 (2001).
4. Adachi, K., Oiwa, K., Nishizaka, T., Furuike, S., Noji, H., Itoh, H., Yoshida, M. & Kinosita, K. Jr. Coupling of rotation and catalysis in F$_1$-ATPase revealed by single-molecule imaging and manipulation. *Cell* **130**, 309–321 (2007).
5. Watanabe, R., Iino, R. & Noji, H. Phosphate release in F$_1$-ATPase catalytic cycle follows ADP release. *Nat. Chem. Biol.* **6**, 814–820 (2010).
6. Laget, P. P. & Smith, J. B. Inhibitory properties of endogenous subunit epsilon in the *Escherichia coli* F$_1$ ATPase. *Arch. Biochem. Biophys.* **197**, 83–89 (1979).
7. Sternweis, P. C. & Smith, J. B. Characterization of the inhibitory epsilon subunit of the proton-translocating adenosine triphosphatase from *Escherichia coli. Biochemistry* **19**, 526–531 (1980).
8. Ort, D. R. & Oxborough, K. *In situ* regulation of chloroplast coupling factor activity. *Annu. Rev. Plant Physiol. Plant Mol. Biol.* **43**, 269–291 (1992).
9. Kato, Y., Matsui, T., Tanaka, N., Muneyuki, E., Hisabori, T. & Yoshida, M. Thermophilic F$_1$-ATPase is activated without dissociation of an endogenous inhibitor, epsilon subunit. *J. Biol. Chem.* **272**, 24906–24912 (1997).
10. Kato-Yamada, Y., Yoshida, M. & Hisabori, T. Movement of the helical domain of the epsilon subunit is required for the activation of thermophilic F$_1$-ATPase. *J. Biol. Chem.* **275**, 35746–35750 (2000).
11. Suzuki, T., Murakami, T., Iino, R., Suzuki, J., Ono, S., Shirakihara, Y. & Yoshida, M. FoF$_1$-ATPase/synthase is geared to the synthesis mode by conformational rearrangement of epsilon subunit in response to proton motive force and ADP/ATP balance. *J. Biol. Chem.* **278**, 46840–46846 (2003).
12. Iino, R., Murakami, T., Iizuka, S., Kato-Yamada, Y., Suzuki, T. & Yoshida, M. Real time monitoring of conformational dynamics of the epsilon subunit in F$_1$-ATPase. *J. Biol. Chem.* **280**, 40130–40134 (2005).
13. Kato, S., Yoshida, M. & Kato-Yamada, Y. Role of the epsilon subunit of thermophilic F$_1$-ATPase as a sensor for ATP. *J. Biol. Chem.* **282**, 37618–37623 (2007).
14. Milgrom, Y. M., Ehler, L. L. & Boyer, P. D. ATP binding at noncatalytic sites of soluble chloroplast F$_1$-ATPase is required for expression of the enzyme activity. *J. Biol. Chem.* **265**, 18725–18728 (1990).
15. Matsui, T., Muneyuki, E., Honda, M., Allison, W. S., Dou, C. & Yoshida, M. Catalytic activity of the alpha3beta3gamma complex of F$_1$-ATPase without noncatalytic nucleotide binding site. *J. Biol. Chem.* **272**, 8215–8221 (1997).
16. Hirono-Hara, Y., Noji, H., Nishiura, M., Muneyuki, E., Hara, K. Y., Yasuda, R., Kinosita, K. Jr. & Yoshida, M. Pause and rotation of F$_1$-ATPase during catalysis. *Proc. Natl. Acad. Sci., USA* **98**, 13649–13654 (2001).
17. Konno, H., Murakami-Fuse, T., Fujii, F., Koyama, F., Ueoka-Nakanishi, H., Pack, C. G., Kinjo, M. & Hisabori, T. The regulator of the F$_1$ motor: inhibition of rotation of cyanobacterial F$_1$-ATPase by the epsilon subunit. *EMBO J.* **25**, 4596–4604 (2006).
18. Feniouk, B. A., Suzuki, T. & Yoshida, M. Regulatory interplay between proton motive force, ADP, phosphate, and subunit epsilon in bacterial ATP synthase. *J. Biol. Chem.* **282**, 764–772 (2007).
19. Tsumuraya, M., Furuike, S., Adachi, K., Kinosita, K. Jr. & Yoshida, M. Effect of epsilon subunit on the rotation of thermophilic *Bacillus* F$_1$-ATPase. *FEBS Lett.* **583**, 1121–1126 (2009).
20. Yasuno, T., Muneyuki, E., Yoshida, M. & Kato-Yamada, Y. Modulation of nucleotide binding to the catalytic sites of thermophilic F$_1$-ATPase by the epsilon subunit: implication for the role of the epsilon subunit in ATP synthesis. *Biochem. Biophys. Res. Commun.* **390**, 230–234 (2009).
21. Hisabori, T., Kato, Y., Motohashi, K., Kroth-Pancic, P., Strotmann, H. & Amano, T. The regulatory functions of the gamma and epsilon subunits from chloroplast CF$_1$ are transferred to the core complex, alpha$_3$beta$_3$, from thermophilic bacterial F1. *Eur. J. Biochem.* **247**, 1158–1165 (1997).
22. Kato-Yamada, Y. & Yoshida, M. Isolated epsilon subunit of thermophilic F$_1$-ATPase binds ATP. *J. Biol. Chem.* **278**, 36013–36016 (2003).
23. Stiggall, D. L., Galante, Y. M. & Hatefi, Y. Preparation and properties of complex V. *Methods Enzymol.* **55**, 308–315 (1979).
24. Bradford, M. M. A rapid and sensitive method for the quantitation of microgram quantities of protein utilizing the principle of protein-dye binding. *Anal. Biochem.* **72**, 248–254 (1976).
25. Nakanishi-Matsui, M., Kashiwagi, S., Hosokawa, H., Cipriano, D. J., Dunn, S. D., Wada, Y. & Futai, M. Stochastic high-speed rotation of *Escherichia coli* ATP synthase F$_1$ sector: the epsilon subunit-sensitive rotation. *J. Biol. Chem.* **281**, 4126–4131 (2006).
26. Dunn, S. D., Zadorozny, V. D., Tozer, R. G. & Orr, L. E. Epsilon subunit of *Escherichia coli* F1-ATPase: effects on affinity for aurovertin and inhibition of product release in unisite ATP hydrolysis. *Biochemistry* **26**, 4488–4493 (1987).
27. Iino, R., Hasegawa, R., Tabata, K. V. & Noji, H. Mechanism of inhibition by C-terminal alpha-helices of the epsilon subunit of *Escherichia coli* FoF$_1$-ATP synthase. *J. Biol. Chem.* **284**, 17457–17464 (2009).